Supplementary materials to the paper in the journal Contributions to Geophysics and Geodesy:

Synthetic 2D GPR constant-offset radargrams: Modelling of responses of air-filled cavities with various shapes

Hamekhani Farhad, Pašteka Roman

Department of engineering geology, hydrogeology and applied geophysics,

Faculty of Sciences, Comenius University, Ilkovičova 6, 842 15 Bratislava

Introduction

In this document we bring results from synthetic modelling of 2D GPR radargrams, which did not fit into the main paper, but we find them interesting and useful. These results are for different types of models, so we have decided to bring them into 4 groups.

Used petrophysical parameters in models

Surrounding dry soil (sand):

relative electric permittivity $\varepsilon_r = 9$, electric conductivity $\sigma = 0.001$ S/m, relative magnetic permeability $\mu_r = 1$.

Air inside the cavity:

relative electric permittivity $\varepsilon_r = 1$, electric conductivity $\sigma = 0$ S/m, relative magnetic permeability $\mu_r = 1$.

Used parameters of the modelled EM field

Frequency of the source of EM waves: 100 MHz.

basic wavelets and modelled components of electric field:

Reflex: Gaussian-like “Cooper” pulse, component E_y,

GPRmax: Ricker wavelet, component E_z,

Irving and Knight: first derivative of a Blackman–Harris window function, component E_y.

1. Group of models: cavity with rectangular cross-section, various vertical dimensions (ReflexW software solutions)

Vertical dimension of the prism is changing from 5 m to 1 m.

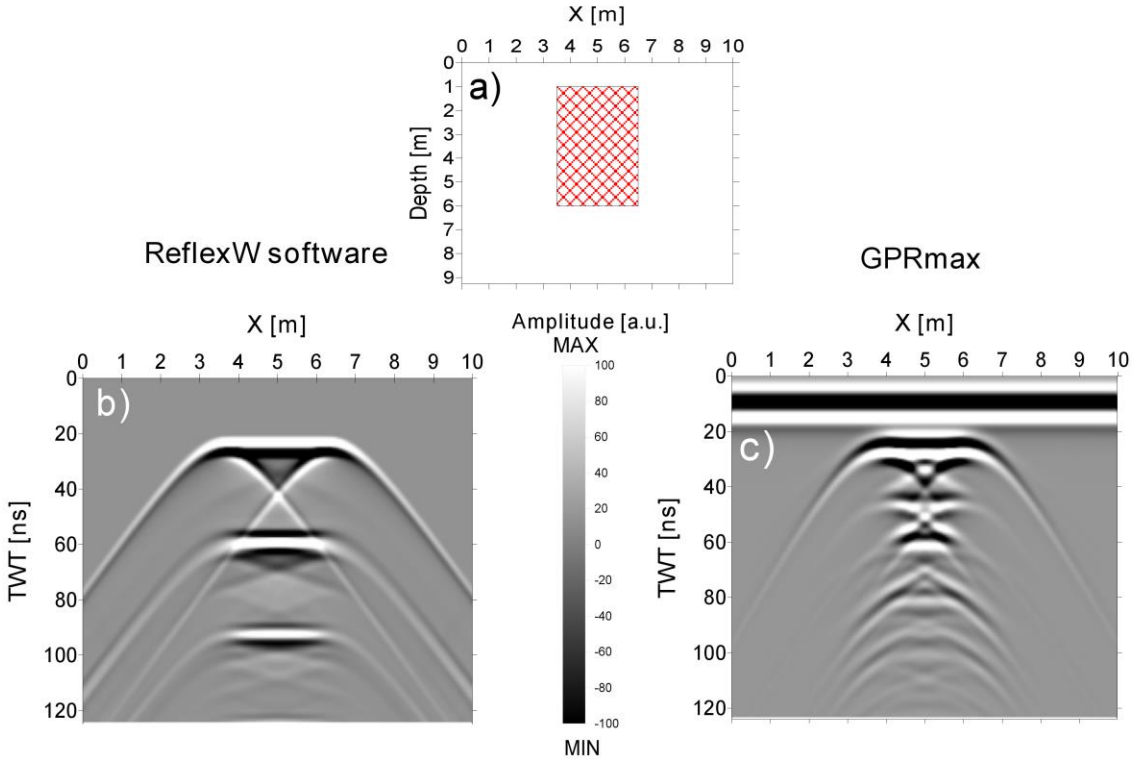

Fig. SM1-1 2D synthetic radargrams of modelled cavity structure with rectangular cross-section (width = 3 m, height = 5 m). Panel a) shows the vertical depth-section of the model; Panel b) shows the original synthetic radargram, calculated with the ReflexW software; Panel c) shows the original synthetic radargram, calculated with the GPRmax software.

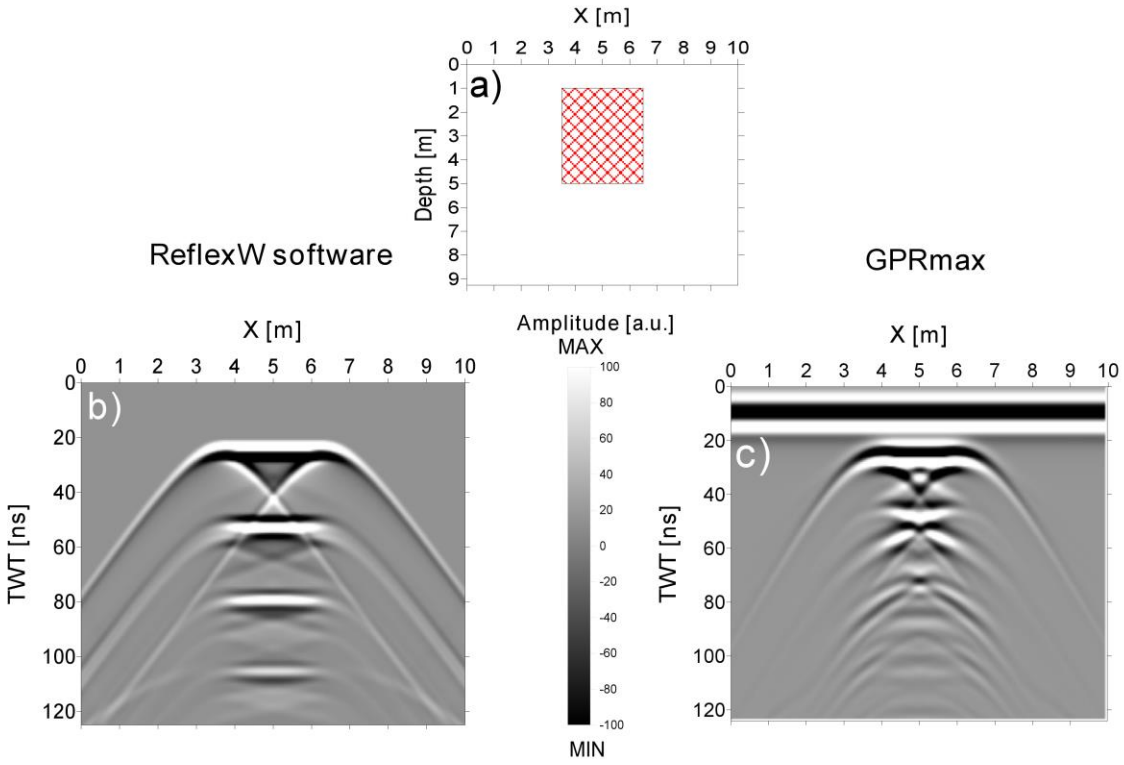

Fig. SM1-2 2D synthetic radargrams of modelled cavity structure with rectangular cross-section (width = 3 m, height = 4 m). Panel a) shows the vertical depth-section of the model; Panel b) shows the original synthetic radargram, calculated with the ReflexW software; Panel c) shows the original synthetic radargram, calculated with the GPRmax software.

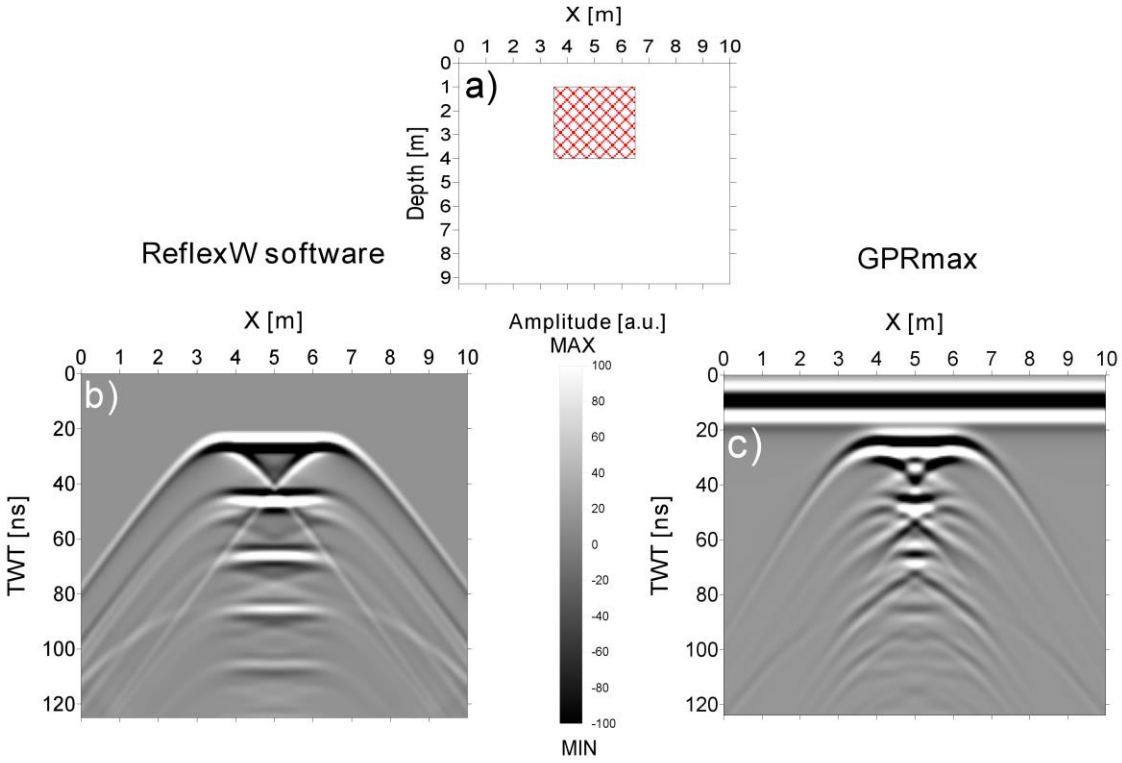

Fig. SM1-3 2D synthetic radargrams of modelled cavity structure with rectangular cross-section (width = 3 m, height = 3 m). Panel a) shows the vertical depth-section of the model; Panel b) shows the original synthetic radargram, calculated with the ReflexW software; Panel c) shows the original synthetic radargram, calculated with the GPRmax software.

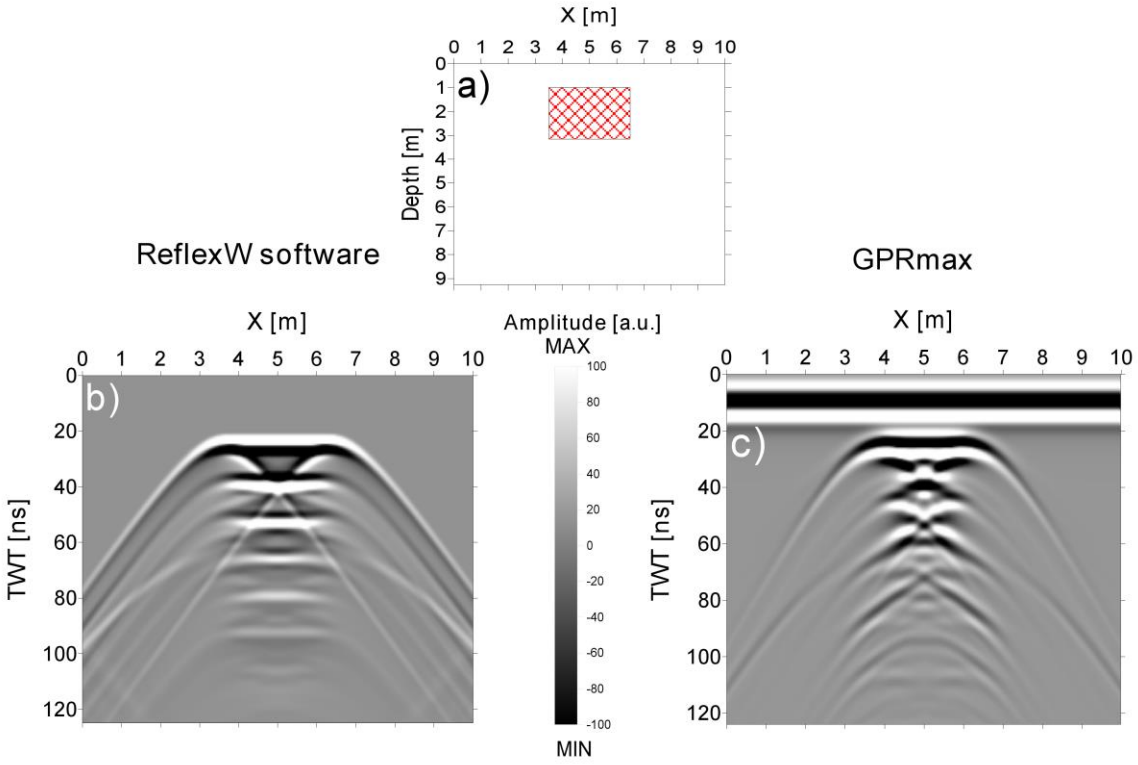

Fig. SM1-4 2D synthetic radargrams of modelled cavity structure with rectangular cross-section (width = 3 m, height = 2 m). Panel a) shows the vertical depth-section of the model; Panel b) shows the original synthetic radargram, calculated with the ReflexW software; Panel c) shows the original synthetic radargram, calculated with the GPRmax software.

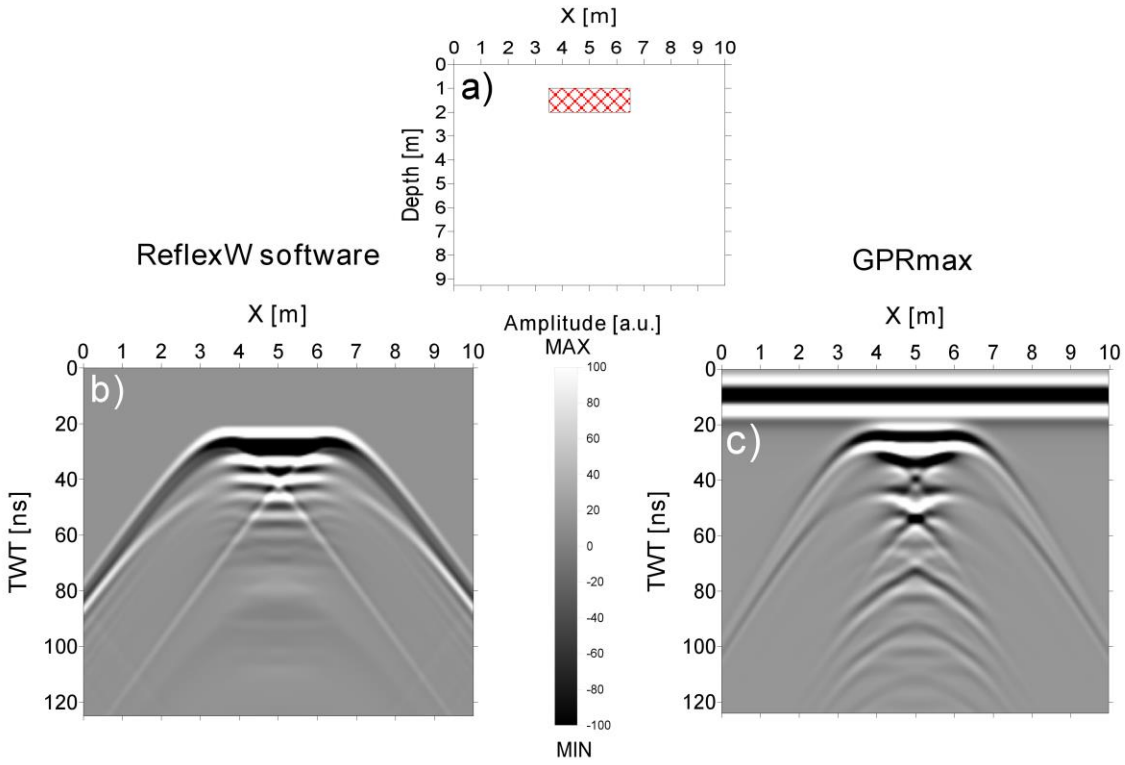

Fig. SM1-5 2D synthetic radargrams of modelled cavity structure with rectangular cross-section (width = 3 m, height = 1 m). Panel a) shows the vertical depth-section of the model; Panel b) shows the original synthetic radargram, calculated with the ReflexW software; Panel c) shows the original synthetic radargram, calculated with the GPRmax software.

2. Group of models: cavity with rectangular cross-section, various horizontal dimensions (ReflexW software solutions)

Horizontal dimension of the prism is changing from 6 m to 0.25 m.

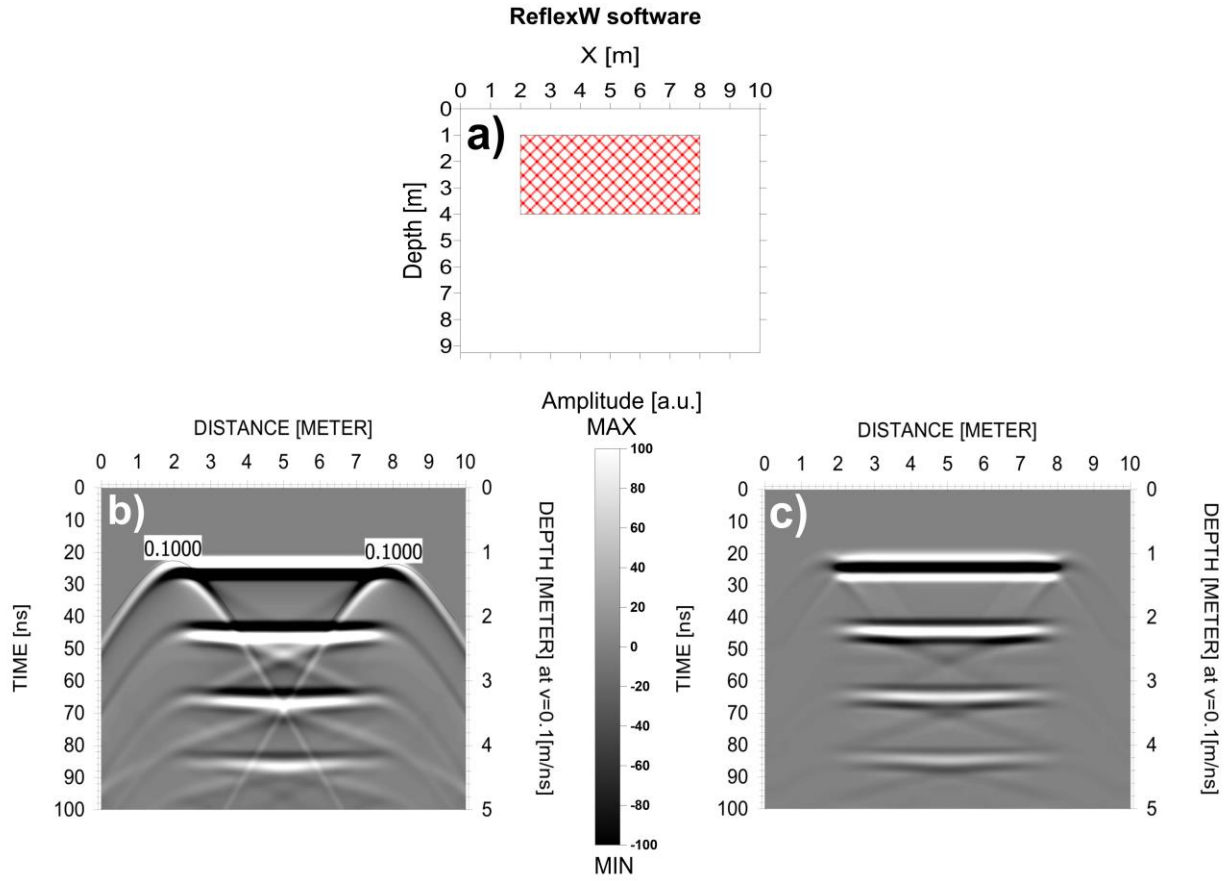

Fig. SM2-1 2D synthetic radargrams of modelled cavity structure with rectangular cross-section (width = 6 m, height = 3 m). Panel a) shows the vertical depth-section of the model; Panel b) shows the original synthetic radargram with interpreted velocity hyperbolas; c) shows the processed synthetic radargram after migration.

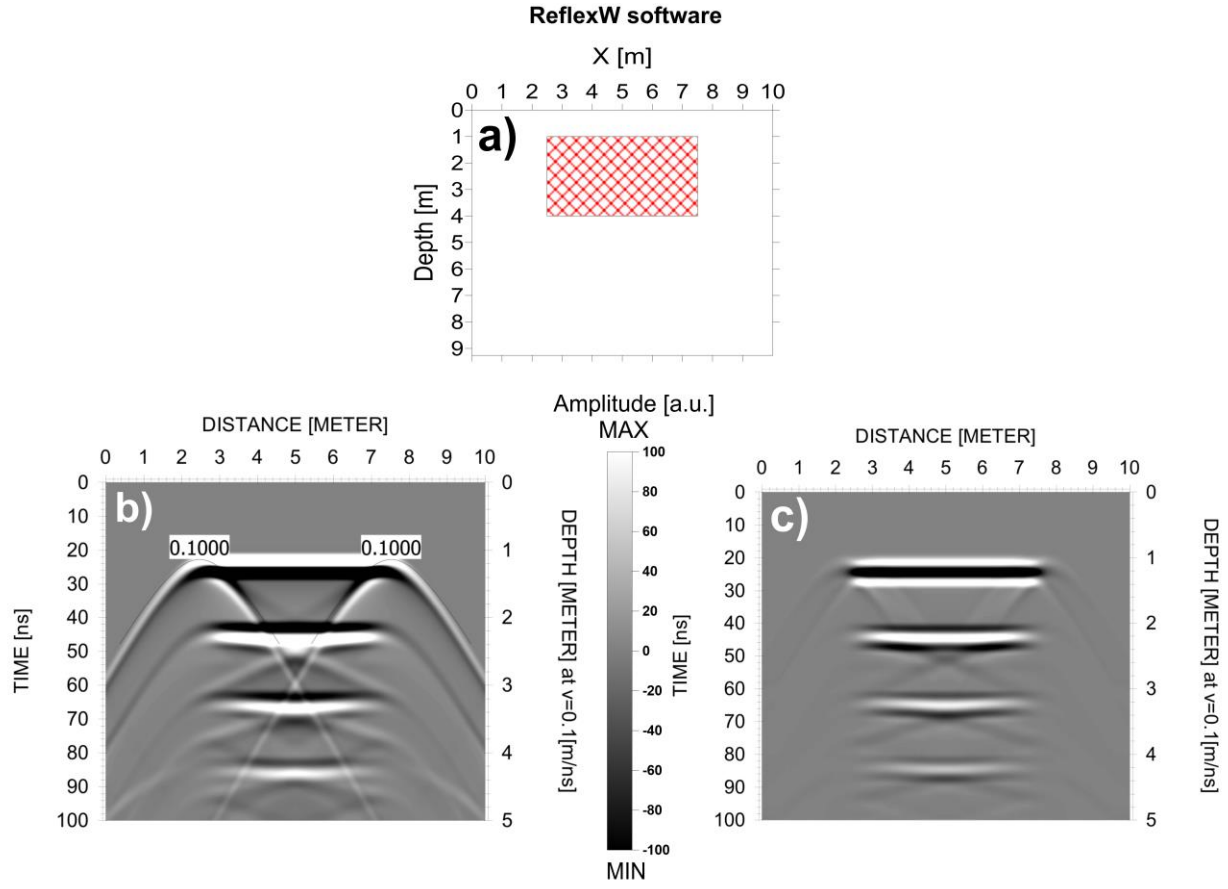

Fig. SM2-2 2D synthetic radargrams of modelled cavity structure with rectangular cross-section (width = 5 m, height = 3 m). Panel a) shows the vertical depth-section of the model; Panel b) shows the original synthetic radargram with interpreted velocity hyperbolas; c) shows the processed synthetic radargram after migration.

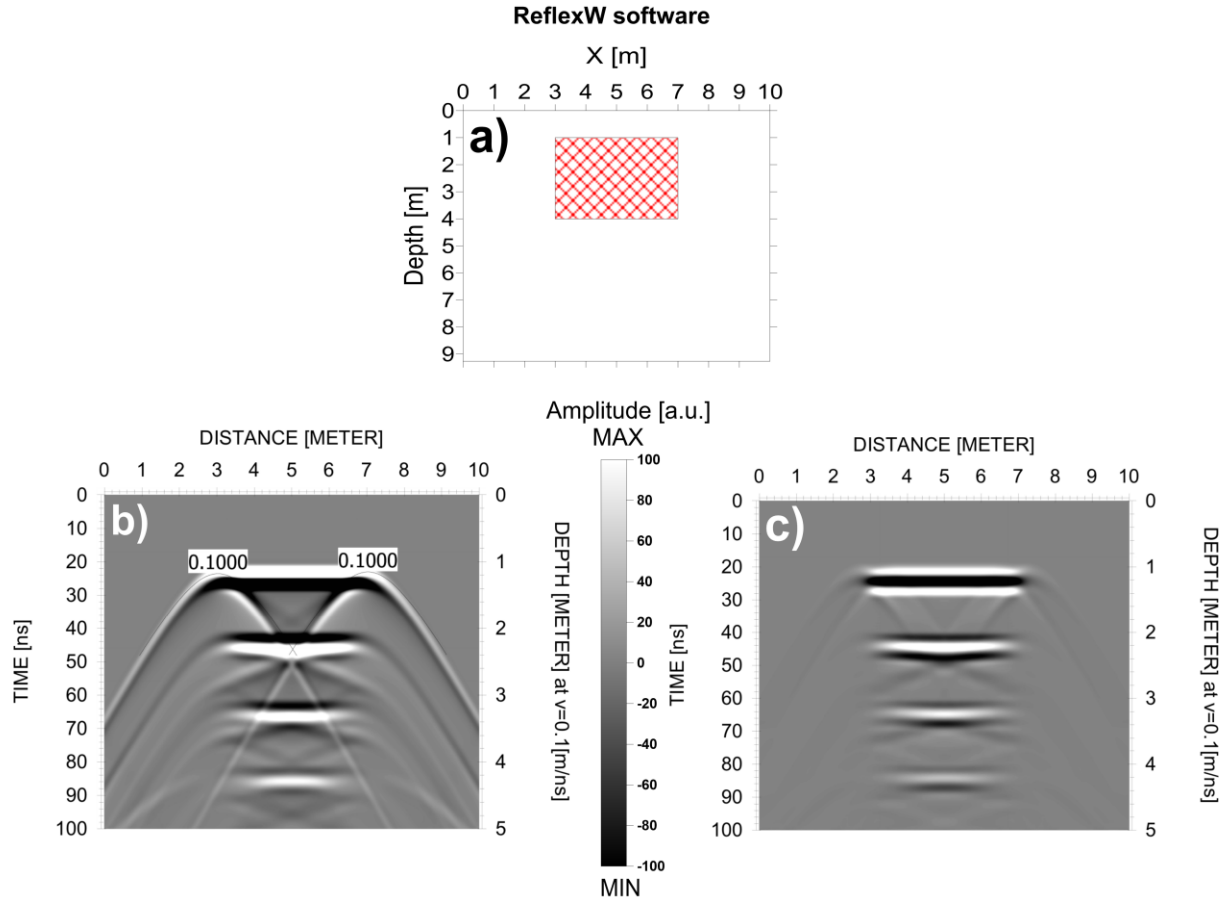

Fig. SM2-3 2D synthetic radargrams of modelled cavity structure with rectangular cross-section (width = 4 m, height = 3 m). Panel a) shows the vertical depth-section of the model; Panel b) shows the original synthetic radargram with interpreted velocity hyperbolas; c) shows the processed synthetic radargram after migration.

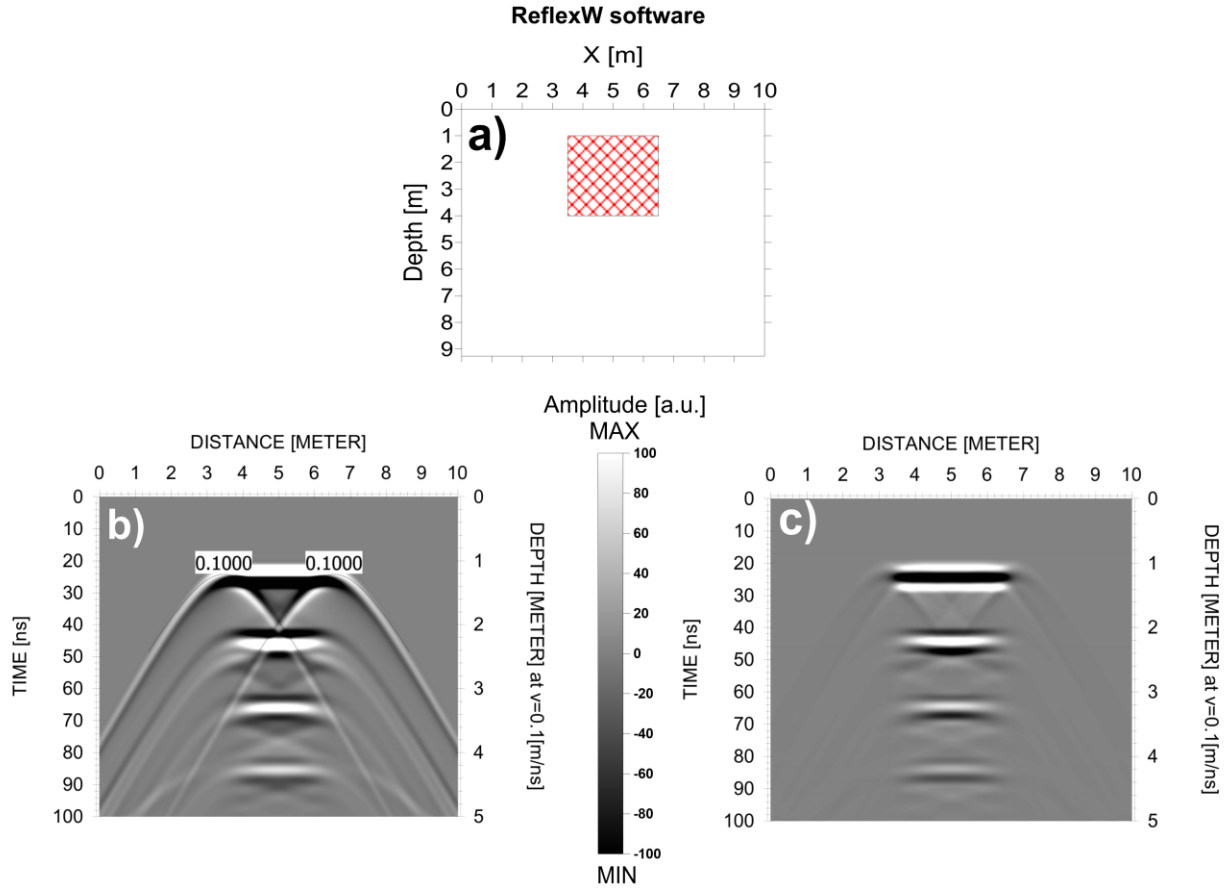

Fig. SM2-4 2D synthetic radargrams of modelled cavity structure with rectangular cross-section (width = 3 m, height = 3 m). Panel a) shows the vertical depth-section of the model; Panel b) shows the original synthetic radargram with interpreted velocity hyperbolas; c) shows the processed synthetic radargram after migration.

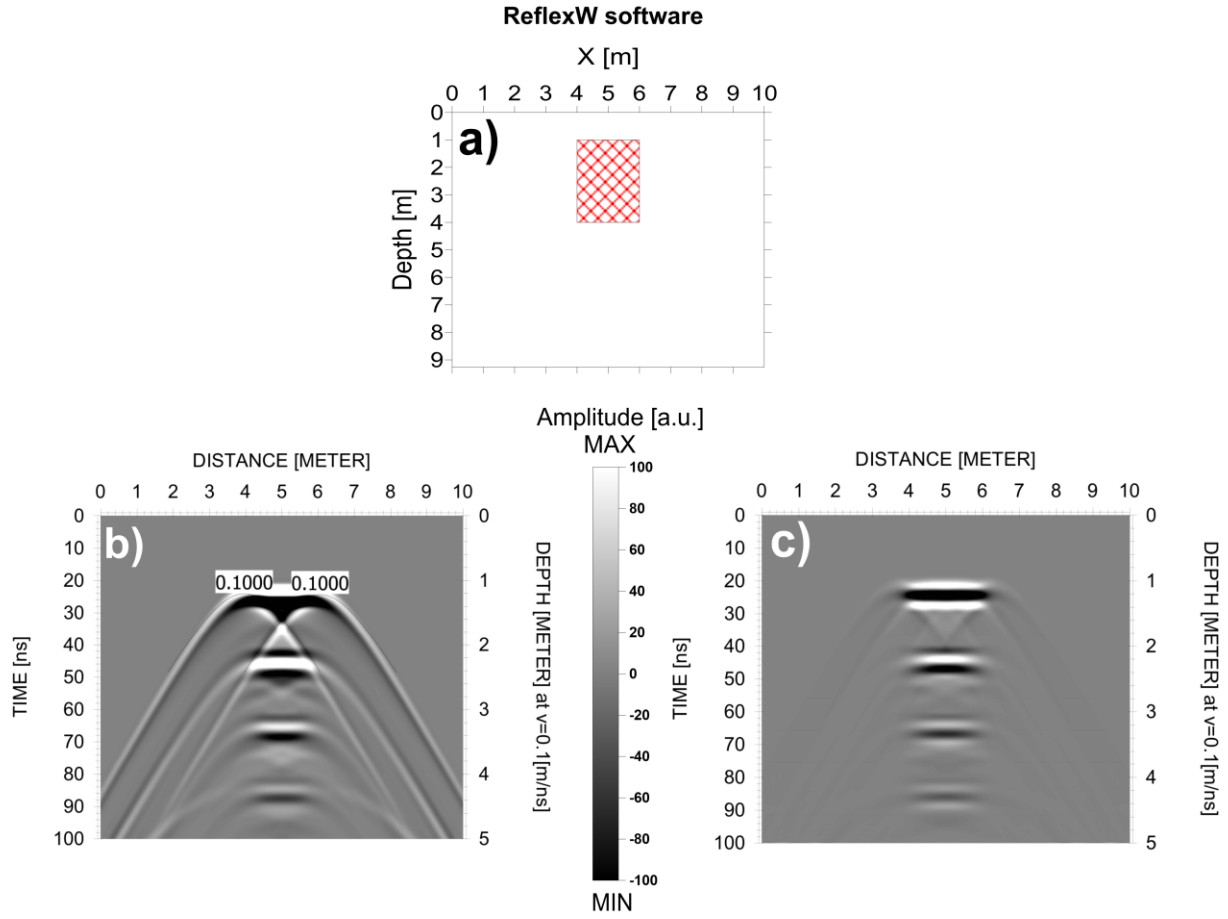

Fig. SM2-5 2D synthetic radargrams of modelled cavity structure with rectangular cross-section (width = 2 m, height = 3 m). Panel a) shows the vertical depth-section of the model; Panel b) shows the original synthetic radargram with interpreted velocity hyperbolas; c) shows the processed synthetic radargram after migration.

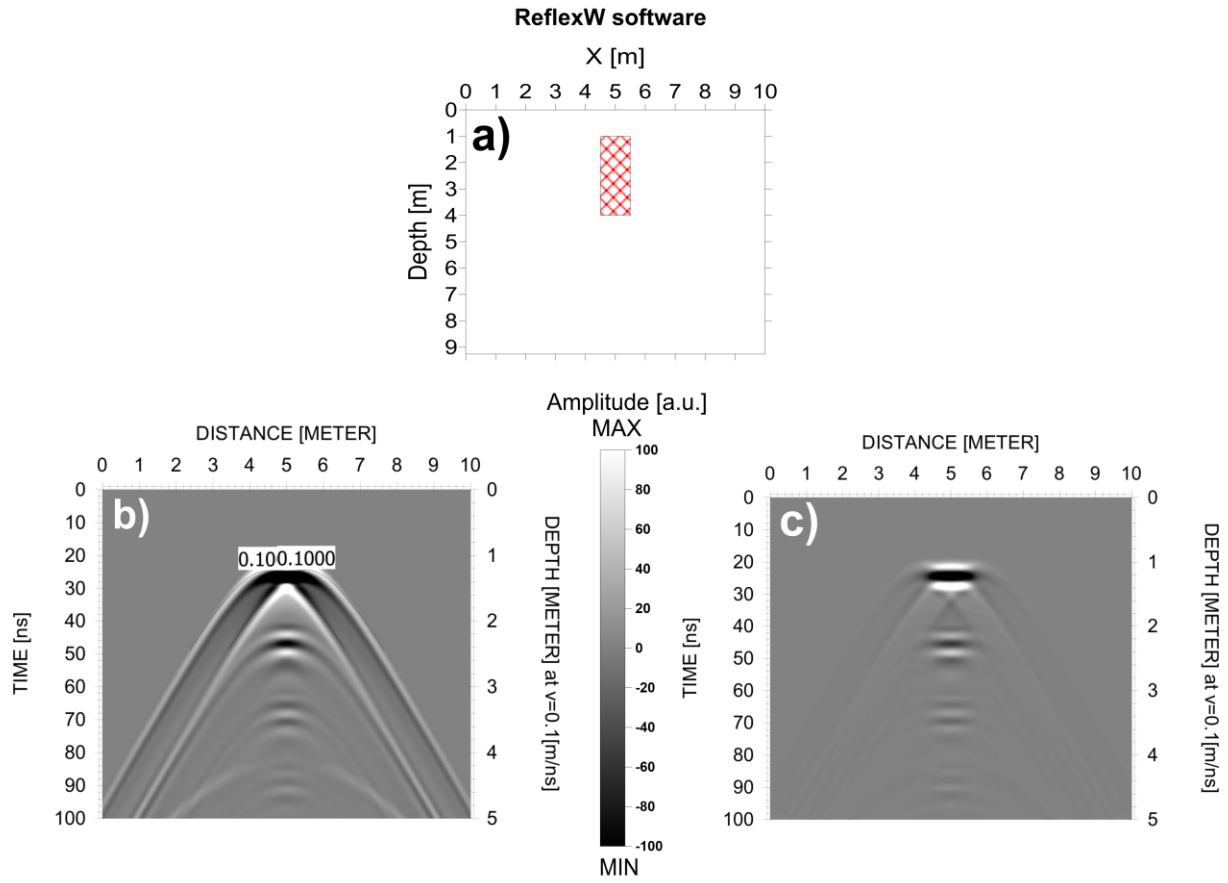

Fig. SM2-6 2D synthetic radargrams of modelled cavity structure with rectangular cross-section (width = 1 m, height = 3 m). Panel a) shows the vertical depth-section of the model; Panel b) shows the original synthetic radargram with interpreted velocity hyperbolas; c) shows the processed synthetic radargram after migration.

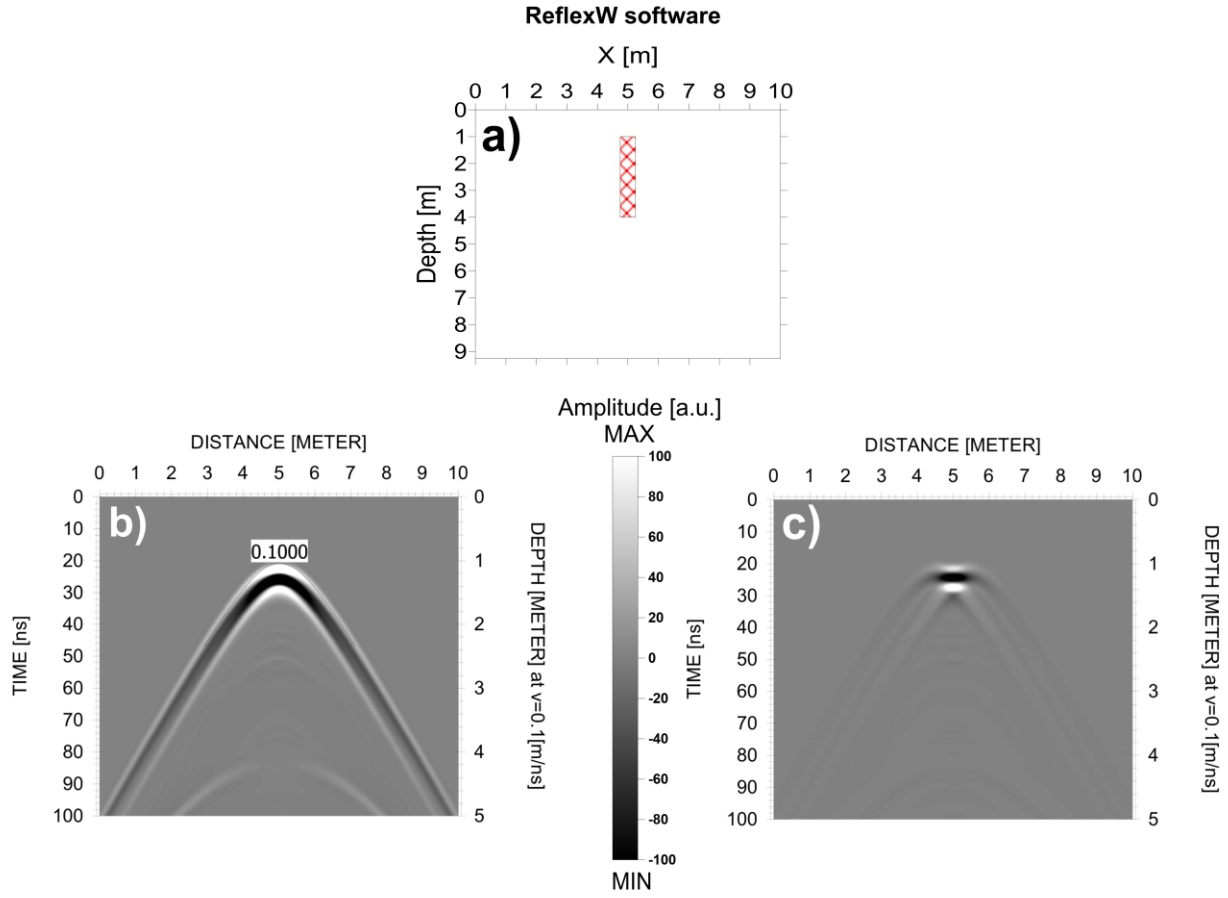

Fig. SM2-7 2D synthetic radargrams of modelled cavity structure with rectangular cross-section (width = 0.5 m, height = 3 m). Panel a) shows the vertical depth-section of the model; Panel b) shows the original synthetic radargram with interpreted velocity hyperbola; c) shows the processed synthetic radargram after migration.

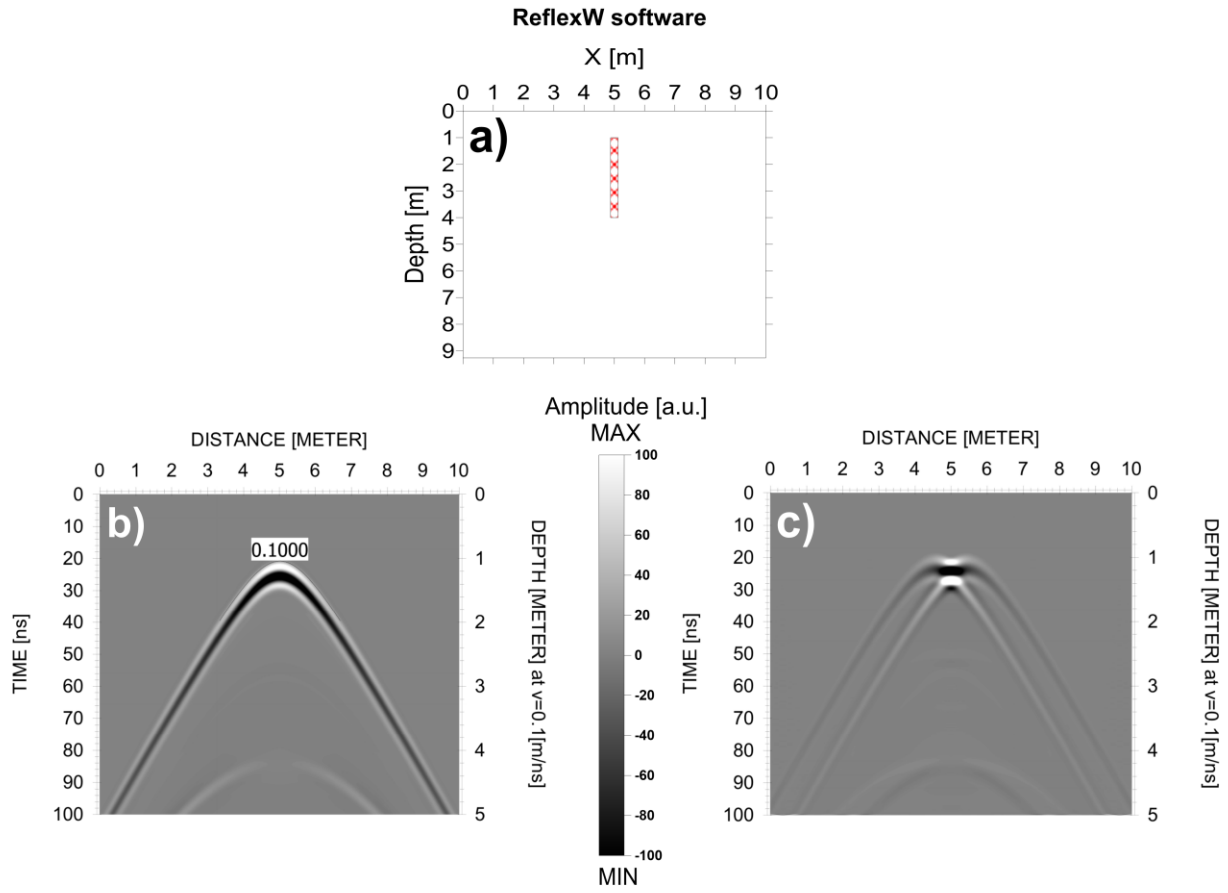

Fig. SM2-8 2D synthetic radargrams of modelled cavity structure with rectangular cross-section (width = 0.25 m, height = 3 m). Panel a) shows the vertical depth-section of the model; Panel b) shows the original synthetic radargram with interpreted velocity hyperbola; c) shows the processed synthetic radargram after migration.

3. Group of models: cavity with normal arched vault, various horizontal dimensions (ReflexW software solutions)

Horizontal dimension of this prism is changing from 2 m to 0.25 m.

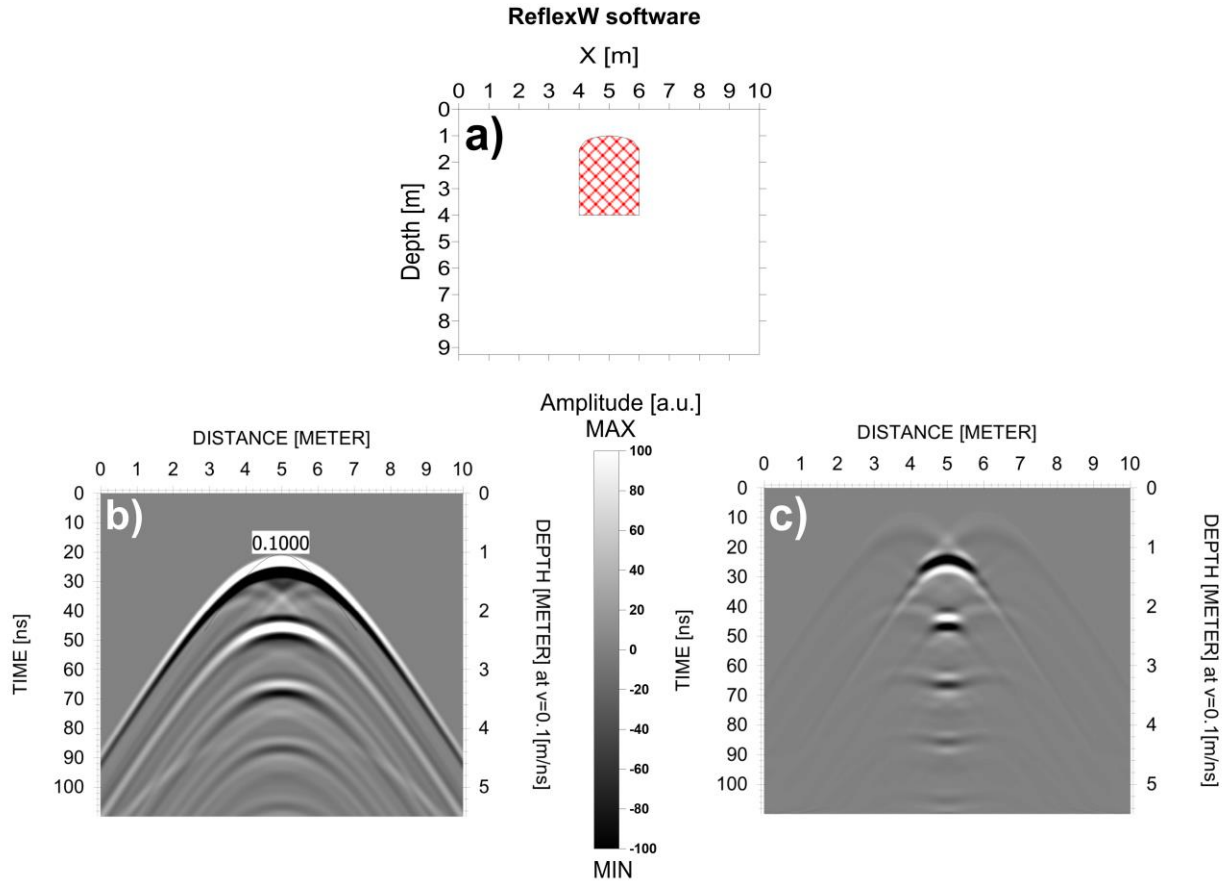

Fig. SM3-1 2D synthetic radargrams of modelled cavity structure with normal arched vault (width = 2 m, height = 3 m). Panel a) shows the vertical depth-section of the model; Panel b) shows the original synthetic radargram with incorrect velocity hyperbola; c) shows the processed synthetic radargram after migration.

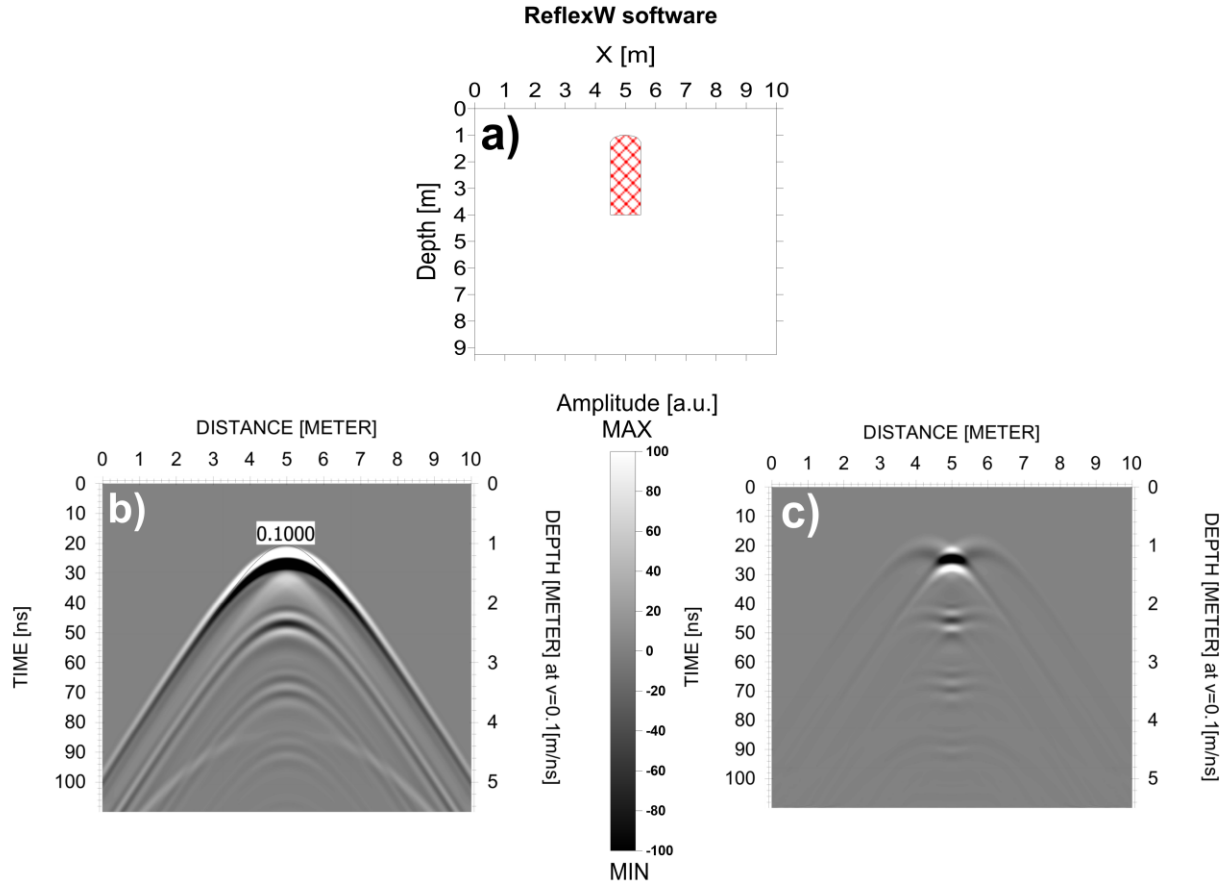

Fig. SM3-2 2D synthetic radargrams of modelled cavity structure with normal arched vault (width = 1 m, height = 3 m). Panel a) shows the vertical depth-section of the model; Panel b) shows the original synthetic radargram with incorrect velocity hyperbola; c) shows the processed synthetic radargram after migration.

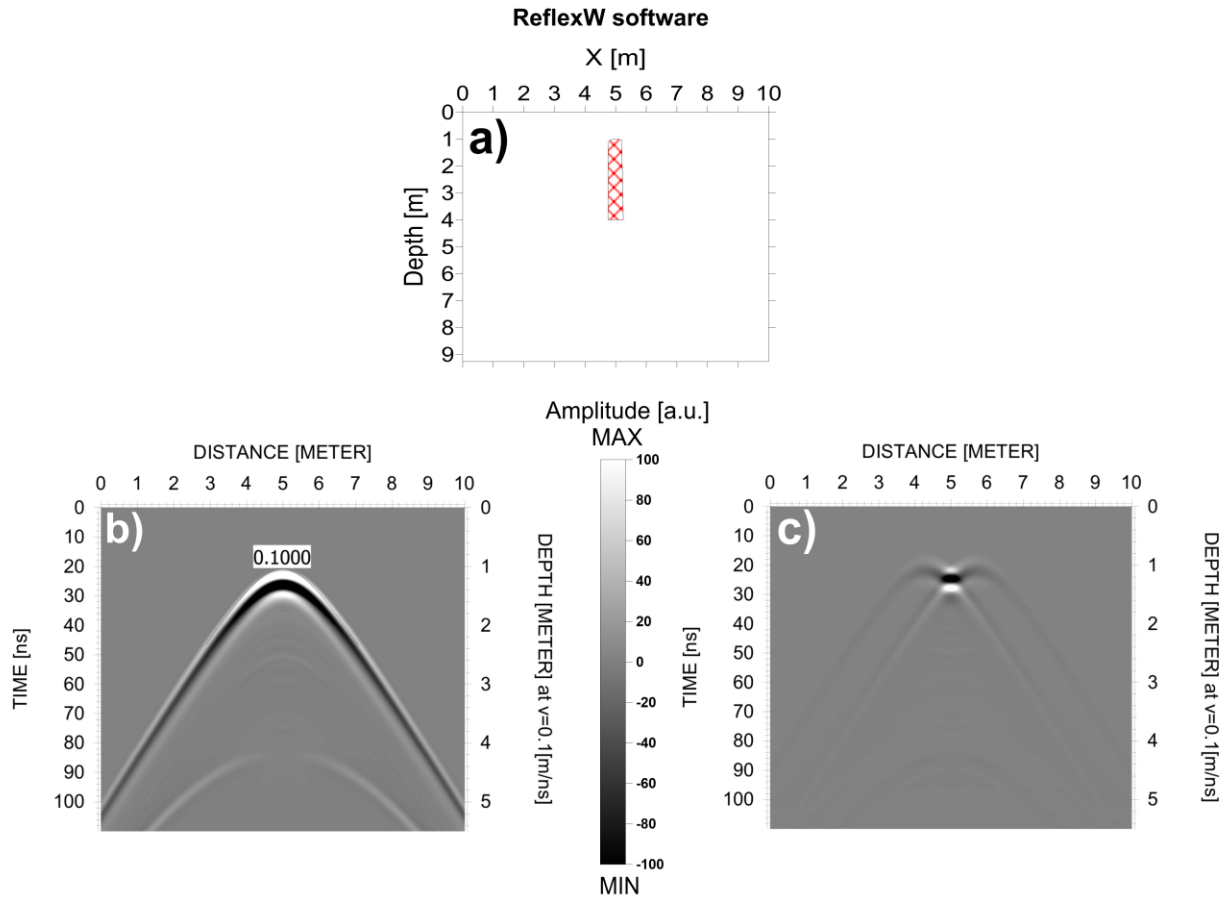

Fig. SM3-3 2D synthetic radargrams of modelled cavity structure with normal arched vault (width = 0.5 m, height = 3 m). Panel a) shows the vertical depth-section of the model; Panels b) shows the original synthetic radargram with interpreted velocity hyperbola; c) shows the processed synthetic radargram after migration.

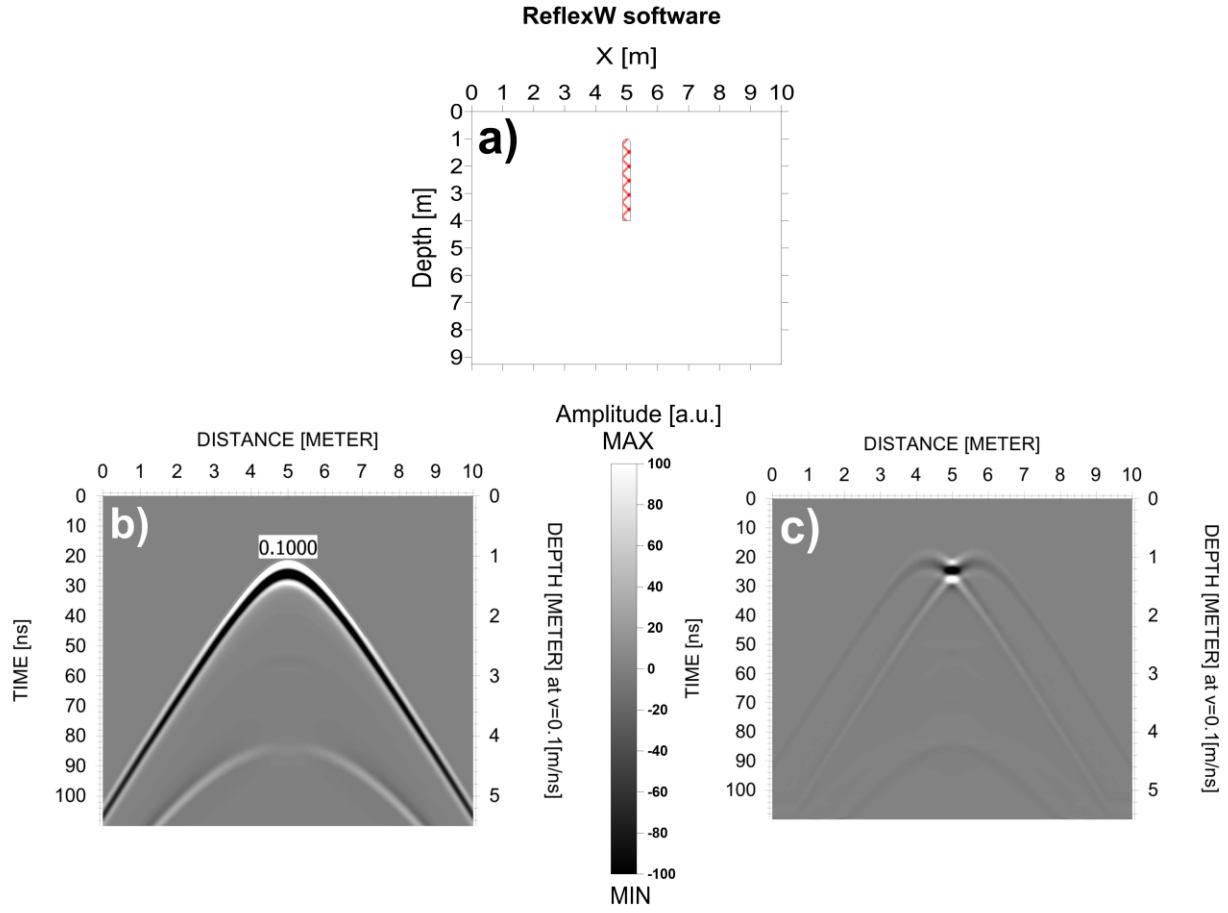

Fig. SM3-4 2D synthetic radargrams of modelled cavity structure with normal arched vault (width = 0.25 m, height = 3 m). Panel a) shows the vertical depth-section of the model; Panel b) shows the original synthetic radargram with interpreted velocity hyperbola; c) shows the processed synthetic radargram after migration.

4. Group of models: models of cavities with various cross-sections (ReflexW software solutions and Irving-Keating method results)

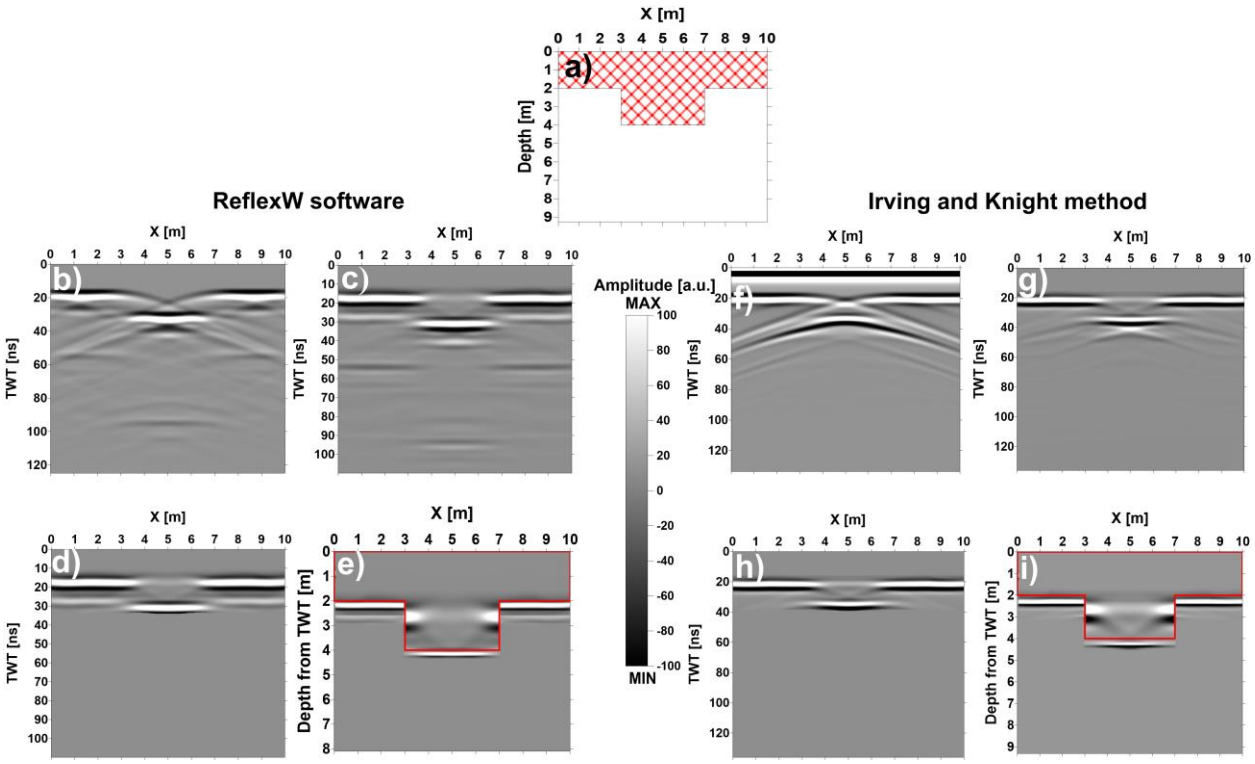

Fig. SM4-1 Comparison of processed 2D synthetic radargrams of modelled cavity structure, simulating a pit with rectangular cross-section. Panel a) shows the vertical depth-section of the model; Panels b) - e) show the results of the ReflexW software: b) the original synthetic radargram, c) migrated version, d) version with removed multiples and e) result from applied CTDC transformation with the outline of the original model (red). Panels f) - i) show the results of the Irwing and Knight method for the same sequence of processing steps as in b) - e). In radargrams g) - i) additional background removal was applied. Red contours in e) and i) show the cross-section of the modelled structure.

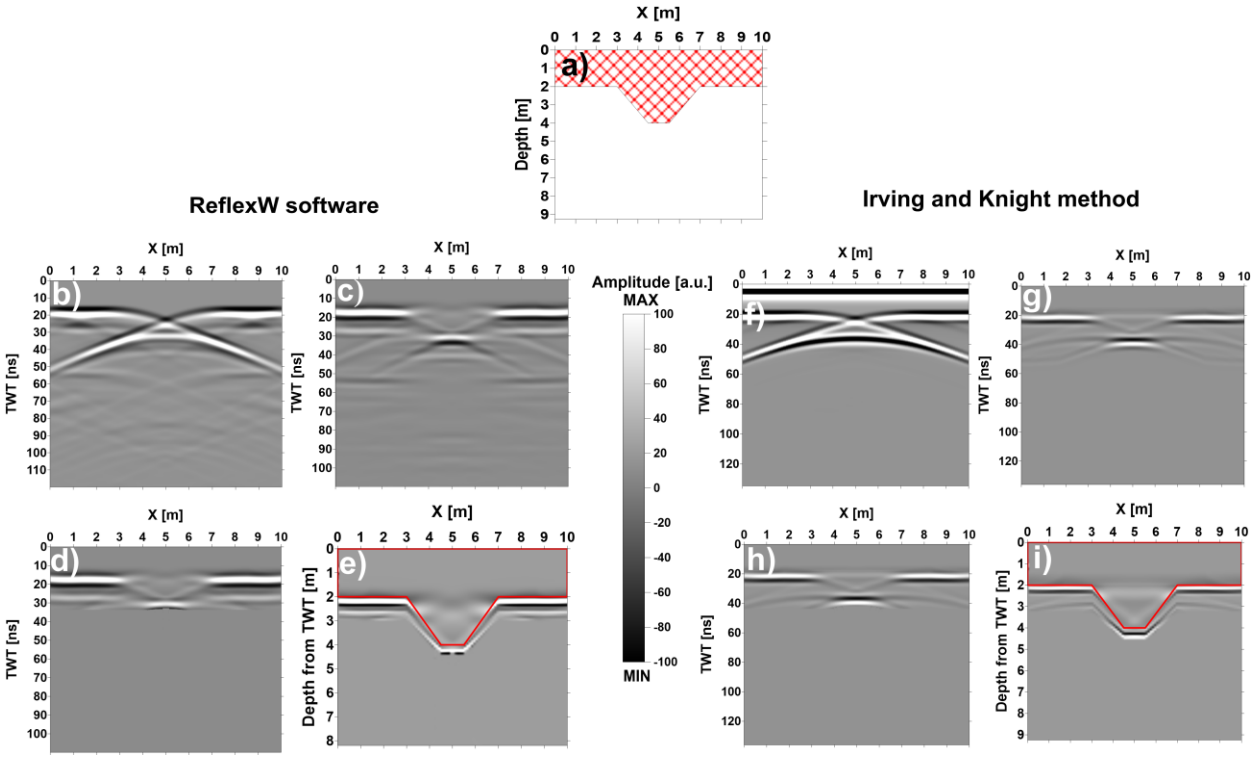

Fig. SM4-2 Comparison of processed 2D synthetic radargrams of modelled cavity structure, simulating a pit with trapezoidal cross-section. Panel a) shows the vertical depth-section of the model; Panels b) - e) show the results of the ReflexW software: b) the original synthetic radargram, c) migrated version, d) version with removed multiples and e) result from applied CTDC transformation with the outline of the original model (red). Panels f) - i) show the results of the Irwing and Knight method for the same sequence of processing steps as in b) - e). In radargrams g) - i) additional background removal was applied. Red contours in e) and i) show the cross-section of the modelled structure.

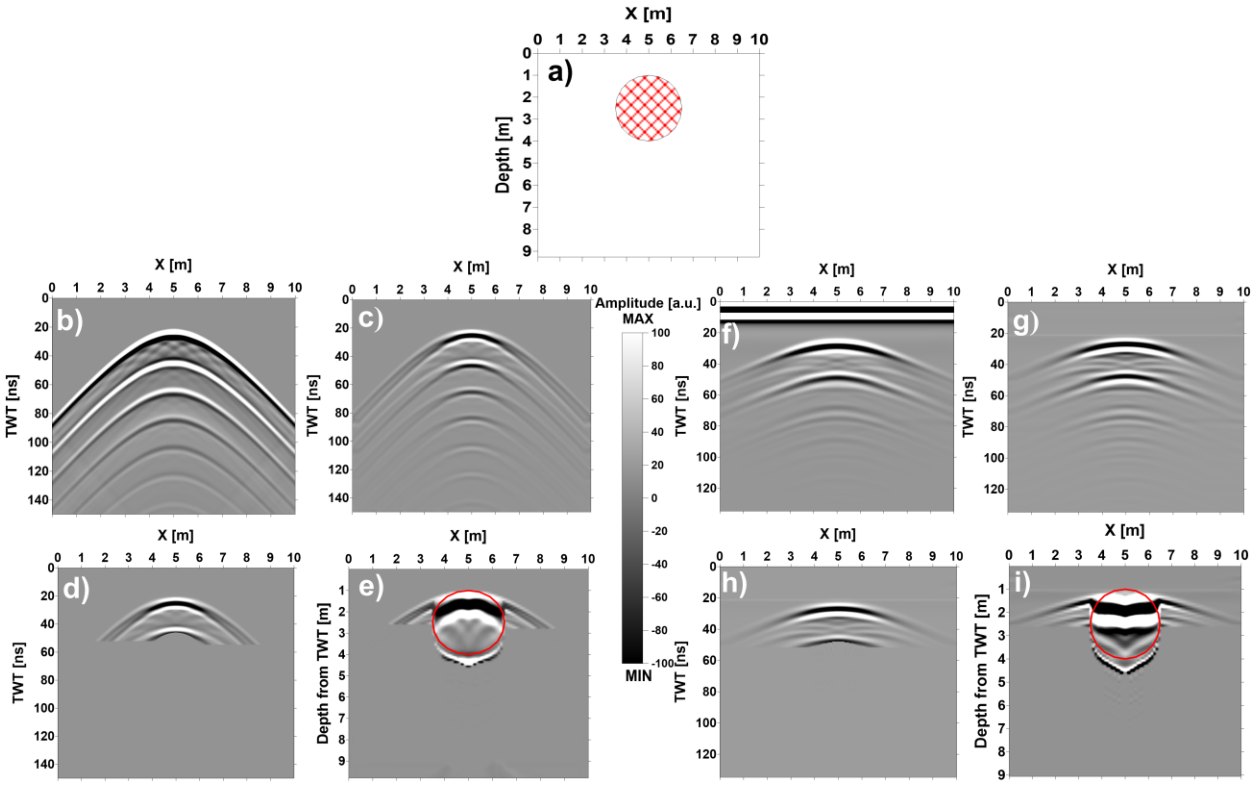

Fig. SM4-3 Comparison of processed 2D synthetic radargrams of modelled cavity with circular cross-section. Panel a) shows the vertical depth-section of the model; Panels b) - e) show the results of the ReflexW software: b) the original synthetic radargram, c) migrated version, d) version with removed multiples and e) result from applied CTDC transformation with the outline of the original model (red). Panels f) - i) show the results of the Irwing and Knight method for the same sequence of processing steps as in b) - e). In radargrams g) - i) additional background removal was applied. Red contours in e) and i) show the cross-section of the modelled structure.

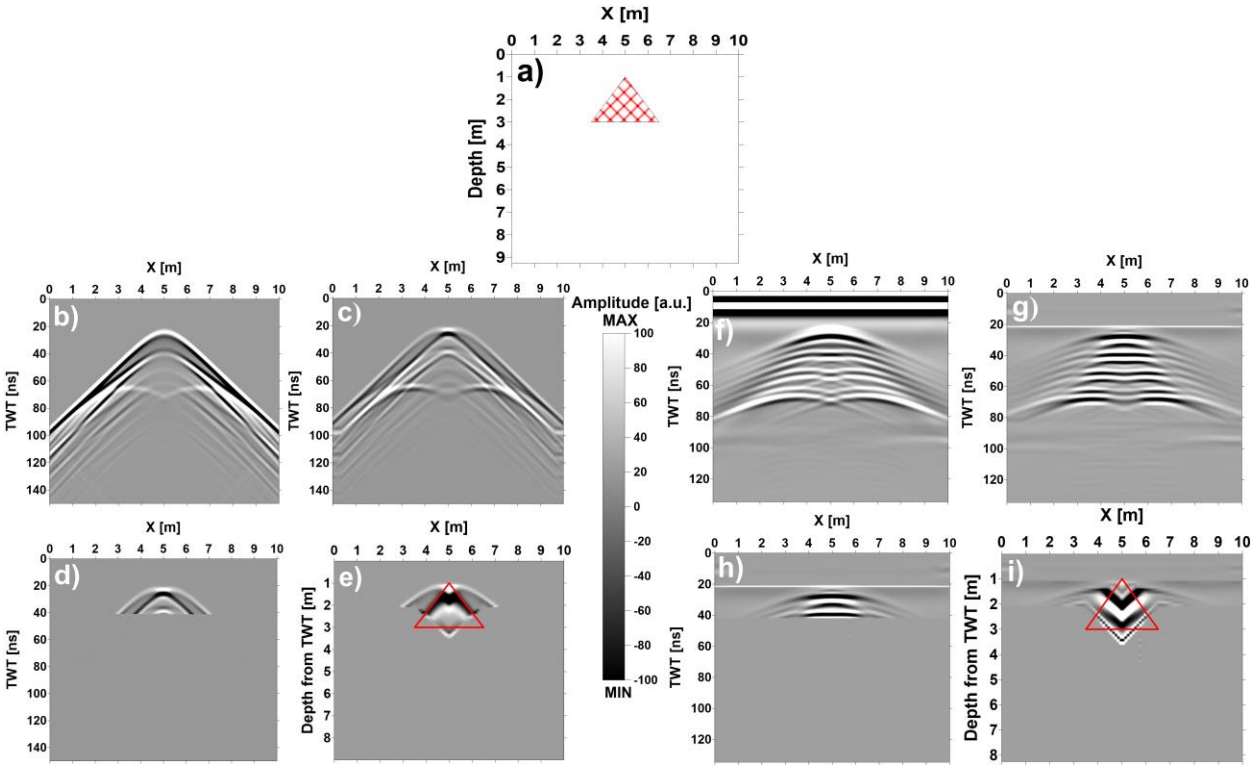

Fig. SM4-4 Comparison of processed 2D synthetic radargrams of modelled cavity with normal triangular cross-section. Panel a) shows the vertical depth-section of the model; Panels b) - e) show the results of the ReflexW software: b) the original synthetic radargram, c) migrated version, d) version with removed multiples and e) result from applied CTDC transformation with the outline of the original model (red). Panels f) - i) show the results of the Irwing and Knight method for the same sequence of processing steps as in b) - e). In radargrams g) - i) additional background removal was applied. Red contours in e) and i) show the cross-section of the modelled structure.

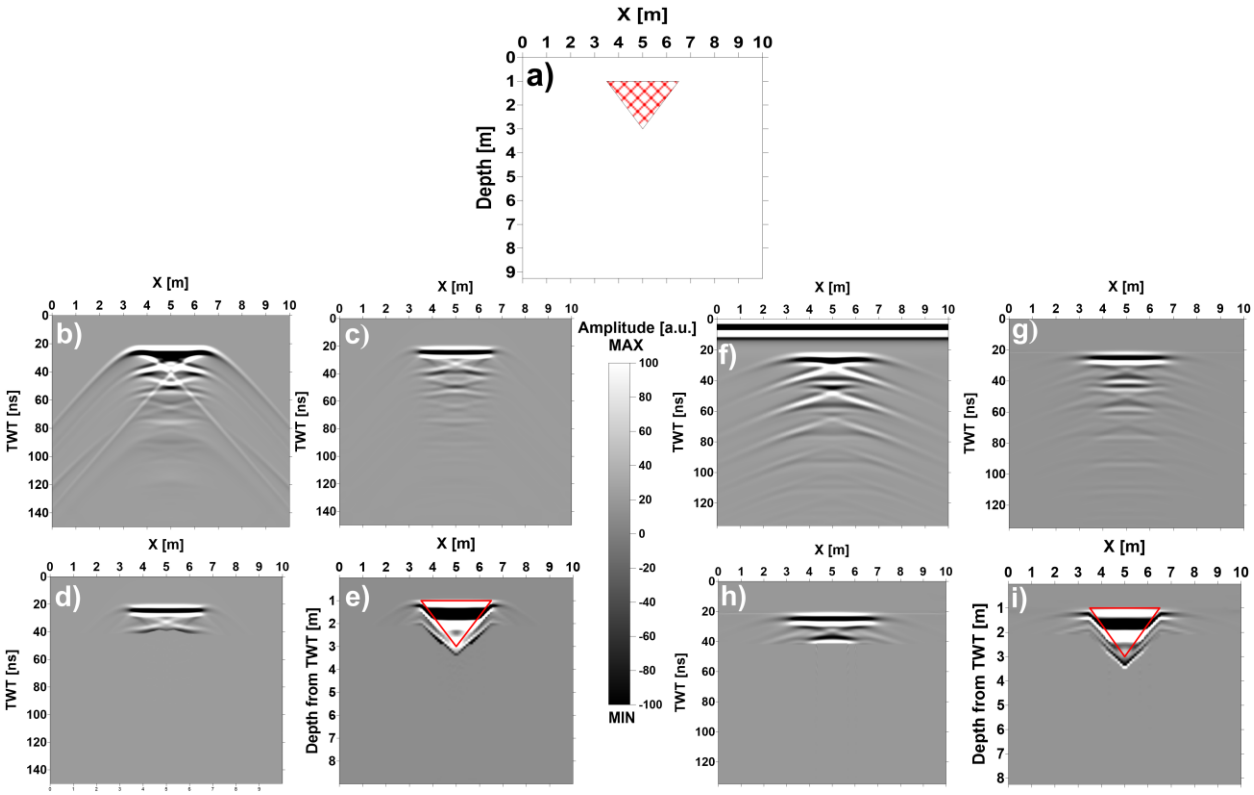

Fig. SM4-5 Comparison of processed 2D synthetic radargrams of modelled cavity with reverse triangular cross-section. Panel a) shows the vertical depth-section of the model; Panels b) - e) show the results of the ReflexW software: b) the original synthetic radargram, c) migrated version, d) version with removed multiples and e) result from applied CTDC transformation with the outline of the original model (red). Panels f) - i) show the results of the Irwing and Knight method for the same sequence of processing steps as in b) - e). In radargrams g) - i) additional background removal was applied. Red contours in e) and i) show the cross-section of the modelled structure.